RSC Advances

PAPER

CrossMark
click for updates

The design of liquid crystalline bistolane-based materials with extremely high birefringence†

Yuki Arakawa,[ab] Sungmin Kang,*[a] Hideto Tsuji,[b] Junji Watanabe[a] and Gen-ichi Konishi*[a]

We designed three new bistolanes with alkylsulfanyl groups. A symmetric derivative contains short terminal methylsulfanyl groups (−SCH₃) on both ends, while two asymmetric derivatives contain a methylsulfanyl group on one end, as well as a highly polarizable cyano (−CN) or isothiocyanate (−NCS) group on the other end. These materials exhibited a well-defined enantiotropic nematic phase, as well as an extremely high birefringence ($\Delta n > 0.6$). Most notably, the NCS derivative achieves an extremely high value of 0.77 at 550 nm. These results should be helpful for the design and synthesis of novel nematic materials with high birefringence.

Introduction

Over the last two decades, liquid crystals (LCs) have attracted substantial attention as materials with high birefringence (Δn). Their intriguing features include self-alignment, anisotropy, and sensitivity to external fields, which provides access to a range of optical and electric materials, as well as display films.[1] So far, these materials have been used extensively as cholesteric (Ch) films,[1c,2] including films for selective and wide reflection, laser emission, holographic applications,[3] and LC lenses.[4] Most high-birefringence LC materials exhibit Δn values of 0.2–0.6. However, in order to improve their performance in the aforementioned applications, values beyond this range are required, as well as thinner LC films and a wider reflection band for circularly polarized light from Ch films. To the best of our knowledge, reports on such materials with $\Delta n > 0.6$ still remain extremely scarce.[5]

The typical design for high-Δn LC materials includes the fabrication of rod-like cores *via* a combination of aromatic rings and/or unsaturated bonds.[3,5,6] High molecular polarizability anisotropies are usually attained by attaching highly polarizable substituents, *e.g.* cyano (−CN) and isothiocyanato (−NCS) groups, to the terminal positions of these compounds.[6]

Recently, we described novel alkylsulfanyl bistolane-based rod-like LC materials, whose mesophases are induced by

introducing a fluorine atom at the lateral position of the central benzene ring.[7] Owing to the S···S interactions and high polarizability of the sulphur atom, these materials exhibit remarkable characteristics, including high Δn and high order parameters. However, various performance-limiting issues remain unresolved. For example, the mesophase range of these materials is narrower compared to that of other derivatives that contain carbon or oxygen atoms.[5a,7,8] Moreover, their Δn values are still lower than those of extremely high-Δn materials, the so-called super-high-Δn (SHB) materials.[5b]

In this study, we present novel bistolane-based LC materials with extremely high Δn ($\Delta n > 0.7$). In order to achieve such extremely high Δn, we aimed to increase the mesophase range and the polarizability anisotropy. Therefore, we designed three bistolane-based LC compounds (Fig. 1): two asymmetric molecules, containing a methylsulfanyl group at one of the terminal positions and a highly polarizable isothiocyanato (**1**) or cyano group (**2**) at the other, as well as a symmetric methylsulfanyl derivative (**3**) with enhanced intermolecular S···S interactions. The present molecular design uses methylsulfanyl groups, *i.e.* the shortest possible alkyl chain, to realize extremely high Δn. Relative to longer alkyl chains, shorter ones should not only lead to a higher density of the mesogenic moiety in direction of
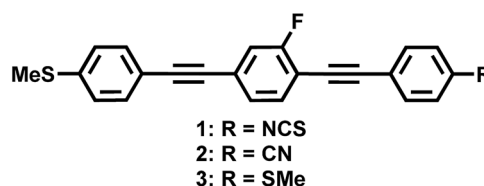
[a]Department of Organic and Polymeric Materials, Tokyo Institute of Technology, O-okayama, Meguro-ku, Tokyo 152-8552, Japan. E-mail: skang@polymer.titech.ac.jp; konishi.g.aa@m.titech.ac.jp

[b]Department of Environmental and Life Sciences, Graduate School of Engineering, Toyohashi University of Technology, Tempaku-cho, Toyohashi, Aichi 441-8580, Japan

† Electronic supplementary information (ESI) available: Synthesis and characterization, DSC chats, POM photos, refractive index, and WAXD measurements. See DOI: 10.1039/c6ra14093a

Fig. 1 Chemical structures of **1**–**3**.

the long molecular axis to provide a high extraordinary refractive index, but also to a wider nematic (N) phase for calamitic LC molecules.
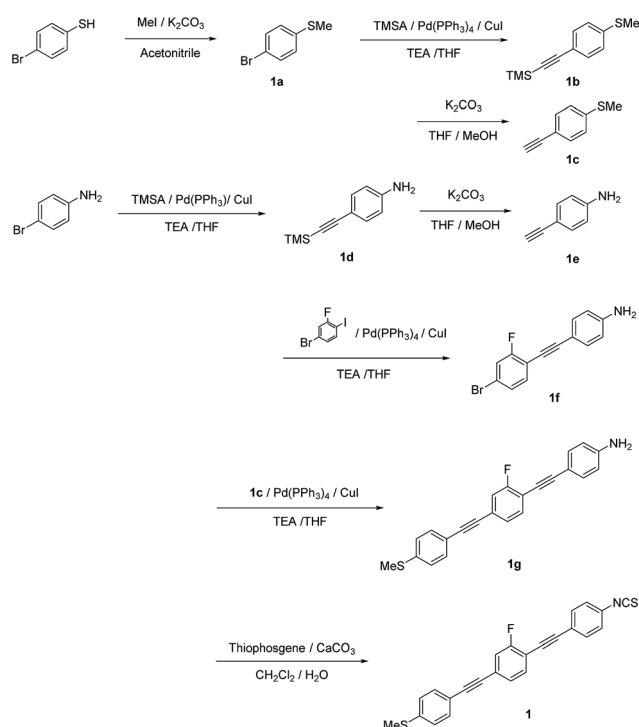
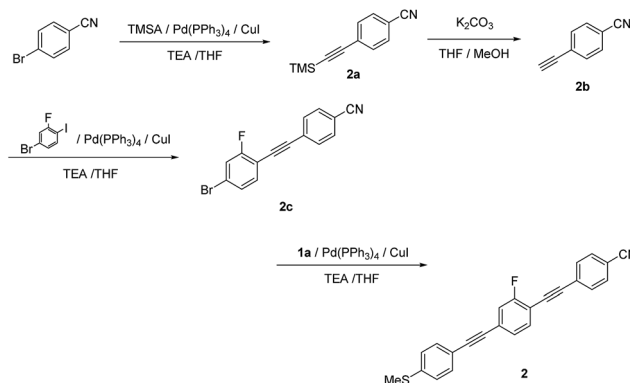## Experimental

Instruments

^{1}H and ^{13}C NMR spectra were measured in CDCl$_3$ on JEOL LNM-EX 400 or Bruker DPX300S spectrometers at room temperature, using tetramethylsilane (TMS) as the internal standard. Liquid crystalline textures were examined by polarizing optical microscopy (POM) on a Leica DM2500P microscopy with a Mettler FP90 hot stage. Transition temperatures and enthalpy changes were measured by differential scanning calorimetry (DSC) on a Perkin Elmer DSC7, whereby heating and cooling scans were carried out using a temperature gradient of 10 °C min^{-1}. Measurements of extraordinary (n_e) and ordinary (n_o) refractive indices and of Δn were carried out in uniaxially aligned nematic cells, which contained an indium tin oxide (ITO) layer and were purchased from EHC. The cell gaps (d) were 2 or 3 μm. The transmittance of light under crossed nicol conditions was observed as a function of wavelength by a microscopic/spectroscopic method using a Nikon LV100 Pol optical microscope equipped with a USB4000 (Ocean photonics) spectrometer.
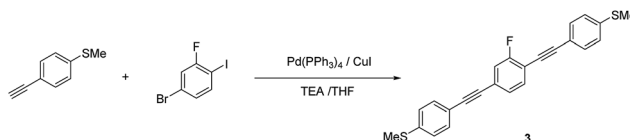
Synthesis

Chemicals were obtained from TCI, Wako, or Nacalai Tesque (Japan) and used as received. The synthetic procedures for all compounds are described and the synthetic routes are shown in Schemes 1–3. The characterization data for **1**–**3** include ^{1}H NMR spectra, as well as high-resolution mass spectrometry (HRMS) data.

Scheme 1 Synthetic route to **1**.

Scheme 2 Synthetic route to **2**.

Scheme 3 Synthetic route to **3**.

Synthesis of 1

*1-Bromo-4-(methylthio)benzene (**1a**).* A mixture of 4-bromo-benzenethiol (7.00 g, 37.0 mmol), iodomethane (MeI; 4.61 mL, 74.0 mmol), K$_2$CO$_3$ (10.2 g, 74.0 mmol), and MeCN (60 mL) was heated to reflux for 12 h. The reaction mixture was cooled to room temperature, extracted with ethyl acetate, washed with water and brine, and dried over MgSO$_4$. After removing the solvent under reduced pressure, **1a** was obtained as a colorless solid (7.41 g, 99%), which was used without further purification. ^{1}H NMR (400 MHz, CDCl$_3$) δ 7.39 (d, J = 8.8 Hz, Ar-H, 2H), 7.12 (d, J = 8.8 Hz, Ar-H, 2H), 2.47 (s, Ar-S–CH_3, 3H) ppm.

*1-Methylthio-4-[2-(trimethylsilyl)ethynyl]benzene (**1b**) (general procedure for Sonogashira coupling).* A mixture of **1a** (7.41 g, 36.5 mmol), Pd(PPh$_3$)$_4$ (0.42 g, 0.37 mmol), CuI (70.0 mg, 0.37 mmol), trimethylsilylacetylene (TMSA; 7.6 mL, 54.7 mmol), triethylamine (TEA; 40 mL), and tetrahydrofuran (THF; 40 mL; degassed by argon sparging) was stirred at 45 °C for 24 h. After cooling to room temperature, the reaction mixture was filtered, extracted with ethyl acetate, washed with aqueous HCl (2 M) and brine, and dried over MgSO$_4$. After evaporating the solvent, the residue was purified by column chromatography on silica gel (eluent: ethyl acetate/hexane = 1/10, v/v) to afford a pale brown oil (7.58 g, 94%). ^{1}H NMR (400 MHz, CDCl$_3$) δ 7.37 (d, J = 8.8 Hz, Ar-H, 2H), 7.15 (d, J = 8.8 Hz, Ar-H, 2H), 2.47 (s, Ar-S–CH_3, 3H), 0.25 (s, Si–(CH$_3$)$_3$, 9H) ppm.

*1-Ethynyl-4-methylthiobenzene (**1c**).* A mixture of **1b** (3.50 g, 15.9 mmol), K$_2$CO$_3$ (4.40 g, 31.8 mmol), MeOH (20 mL), and THF (20 mL) was stirred at room temperature for 30 min. Then, the reaction mixture was extracted with ethyl acetate and washed with brine. After evaporating the solvent, **1c** was obtained as a colorless solid (0.72 g, >99%). ^{1}H NMR (400 MHz,

CDCl$_3$) δ 7.40 (d, J = 8.4 Hz, Ar-H, 2H), 7.17 (d, J = 8.4 Hz, Ar-H, 2H), 3.07 (s, C≡C–H, 1H), 2.48 (s, Ar-S–CH$_3$, 3H) ppm.

4-[2-(Trimethylsilyl)ethynyl]aniline (1d). Compound **1d** was synthesized according to the generic Sonogashira coupling conditions outlined for the preparation of **1b**: 4-iodoaniline (8.00 g, 36.5 mmol), trimethylsilylacetylene (7.58 mL, 54.8 mmol), TEA (40 mL), THF (40 mL), Pd(PPh$_3$)$_4$ (0.420 g, 0.365 mmol), and CuI (69.5 mg, 0.365 mmol). Purification by column chromatography on silica gel (eluent: ethyl acetate/ hexane = 1/3, v/v) afforded **1d** as a pale brown solid in 77% yield. ^{1}H NMR (300 MHz, CDCl$_3$) δ 7.23 (d, J = 8.4 Hz, Ar-H, 2H), 6.57 (d, J = 8.4 Hz, Ar-H, 2H), 3.79 (brs, –NH$_2$, 2H), 0.23 (s, Si–(CH$_3$)$_3$, 9H) ppm.

4-Ethynylaniline (1e). Compound **1e** was synthesized according to the method for the deprotection of trimethylsilyl groups used for the preparation of **1c**: **1d** (5.27 g, 27.8 mmol), K$_2$CO$_3$ (5.77 g, 41.8 mmol), MeOH (30 mL), and THF (30 mL). Yield: 99%. Pale brown solid. ^{1}H NMR (300 MHz, CDCl$_3$) δ 7.30 (d, J = 8.4 Hz, Ar-H, 2H), 6.60 (d, J = 8.4 Hz, Ar-H, 2H), 2.96 (s, C≡C–H, 1H) ppm.

4-[2-(4-Bromo-2-fluorophenyl)ethynyl]aniline (1f). Compound **1f** was synthesized according to the generic Sonogashira coupling conditions outlined for the preparation of **1b**: **1e** (3.26 g, 27.8 mmol), 4-bromo-2-fluoroiodobenzene (10.0 g, 33.4 mmol), TEA (40 mL), THF (40 mL), Pd(PPh$_3$)$_4$ (0.320 g, 0.280 mmol), and CuI (53.0 mg, 0.280 mmol). Purification by column chromatography on silica gel (eluent: ethyl acetate/hexane = 1/ 3, v/v) afforded **1f** as a colorless solid in 77% yield. ^{1}H NMR (300 MHz, CDCl$_3$) δ 7.35 (d, J = 8.1 Hz, Ar-H, 2H), 7.33-7.22 (m, Ar-H, 3H), 6.64 (d, J = 8.1 Hz, Ar-H, 2H), 3.87 (brs, –NH$_2$, 2H) ppm.

2-Fluoro-1-[2-(4-aminophenyl)ethynyl]-4-[2-(4-thiophenyl) ethynyl]benzene (1g). Compound **1g** was synthesized according to the generic Sonogashira coupling conditions outlined for the preparation of **1b**: **1c** (0.34 g 2.27 mmol), **1f** (0.66 g, 2.27 mmol), TEA (5 mL), THF (5 mL), Pd(PPh$_3$)$_4$ (0.13 g, 0.11 mmol), and CuI (21 mg, 0.11 mmol). Purification by column chromatography on silica gel (eluent: chloroform/hexane = 1/2, v/v) afforded **1g** as a pale yellow solid in 27% yield. ^{1}H NMR (300 MHz, CDCl$_3$) δ 7.46–40 (m, Ar-H, 3H), 7.36 (d, J = 8.4 Hz, Ar-H, 2H), 7.25–7.17 (m, Ar-H, 4H), 6.65 (d, J = 8.1 Hz, Ar-H, 2H), 3.86 (brs, –NH$_2$, 2H), 2.50 (s, –CH$_3$, 3H) ppm.

2-Fluoro-1-[2-(4-isothiocyanatophenyl)ethynyl]-4-[2-(4-methyl-thiophenyl)ethynyl]benzene (1). A mixture of **1g** (0.650 g, 1.82 mmol), CaCO$_3$ (0.360 g, 3.64 mmol), dichloromethane (25 mL), and water (10 mL) was cooled to 0 °C. Then, thiophosgene (0.19 mL, 2.52 mmol) was added dropwise, and the resulting mixture was stirred for 12 h at room temperature. Subsequently, the mixture was extracted with CHCl$_3$, washed with water and brine, and dried over MgSO$_4$. After removing all volatiles, the residue was purified by column chromatography on silica gel (eluent: chloroform/hexane = 1/2, v/v). The residue was recrystallized from CHCl$_3$ and hexane to afford the target compound as a pale brown solid in 77%. ^{1}H NMR (300 MHz, CDCl$_3$) δ 7.55 (d, J = 8.4 Hz, Ar-H, 2H), 7.51–7.41 (m, Ar-H, 3H), 7.30 (d, J = 8.4 Hz, Ar-H, 2H), 7.24 (d, J = 8.4 Hz, Ar-H, 4H), 2.53 (s, –CH$_3$, 3H) ppm. HRMS-FAB$^+$ (m/z): [M]$^+$ calcd for C$_{24}$H$_{14}$FNS$_2$, 399.0552; found, 399.0556.

Synthesis of 2

1-Cyano-4-[2-(trimethylsilyl)ethynyl]benzene (2a). Compound **2a** was synthesized according to the general Sonogashira coupling conditions outlined for the preparation of **1b**: 4-bromobenzonitrile (5.00 g, 27.5 mmol), trimethylsilylacetylene (5.70 mL, 41.2 mmol), TEA (20 mL), THF (20 mL), Pd(PPh$_3$)$_4$ (0.320 g, 0.275 mmol), and CuI (52.3 mg, 0.275 mmol); purification by column chromatography on silica gel (eluent: CHCl$_3$/hexane = 1/ 6, v/v); yield: >99%; pale yellow solid. ^{1}H NMR (300 MHz, CDCl$_3$) δ 7.59 (d, J = 8.4 Hz, Ar-H, 2H), 7.53 (d, J = 8.4 Hz, Ar-H, 2H), 3.07 (s, C≡C–H, 1H), 0.28 (s, Si–(CH$_3$)$_3$, 9H) ppm.

1-Cyano-4-ethynylbenzene (2b). Compound **2b** was synthesized according to the general method for the deprotection of trimethylsilyl groups used for the preparation of **1c**: **2a** (5.48 g, 27.5 mmol), K$_2$CO$_3$ (11.4 g, 82.5 mmol), MeOH (40 mL), and THF (40 mL); yield: 54%; colorless solid. ^{1}H NMR (300 MHz, CDCl$_3$) δ 7.62 (d, J = 8.4 Hz, Ar-H, 2H), 7.57 (d, J = 8.4 Hz, Ar-H, 2H), 3.30 (s, C≡C–H, 1H) ppm.

4-[2-(4-Bromo-2-fluorophenyl)ethynyl]benzonitrile (2c). Compound **2c** was synthesized according to the general Sonogashira coupling conditions used for the preparation of **1b**: 4-ethynylbenzonitrile (0.900 g, 7.08 mmol), 4-bromo-2-fluoroiodobenzene (2.55 g, 8.49 mmol), TEA (15 mL), THF (15 mL), Pd(PPh$_3$)$_4$ (0.245 g, 0.212 mmol), and CuI (40.4 mg, 0.212 mmol); purification by column chromatography on silica gel (eluent: CHCl$_3$/hexane = 1/3, v/v); yield: 86%; colorless solid. ^{1}H NMR (300 MHz, CDCl$_3$) δ 7.66 (d, J = 8.7 Hz, Ar-H, 2H), 7.62 (d, J = 8.7 Hz, Ar-H, 2H), 7.42–7.29 (m, Ar-H, 3H) ppm, ^{13}C NMR (300 MHz) δ 86.4, 94.0 (d, J = 3.7 Hz), 110.5, 110.7, 112.5, 118.8, 119.8, 120.1, 124.1 (d, J = 9.0 Hz), 127.8, 128.1 (d, J = 3.7 Hz), 132.5 (d, J = 3.0 Hz), 132.5 (d, J = 3.0 Hz), 134.6 (d, J = 1.5 Hz), 161.1, 164.5 ppm.

2-Fluoro-1-[2-(4-cyanophenyl)ethynyl]-4-[2-(4-methylthiophenyl) ethynyl]benzene (2). Compound **2** was synthesized according to the general Sonogashira coupling conditions used for the preparation of **1b**: **2c** (0.100 g, 0.330 mmol), **1c** (53.0 mg, 0.360 mmol), TEA (5 mL), THF (5 mL), Pd(PPh$_3$)$_4$ (19.0 mg, 17.0 μmol), and CuI (3.10 mg, 17.0 μmol); purification by column chromatography on silica gel (eluent: CHCl$_3$/hexane = 1/2, v/v), followed by recrystallisation from CHCl$_3$/hexane; yield: 82%; colorless solid; ^{1}H NMR (400 MHz, CDCl$_3$) δ 7.66 (d, J = 8.4 Hz, Ar-H, 2H), 7.63 (d, J = 8.8 Hz, Ar-H, 2H), 7.48 (s, Ar-H, 1H), 7.44 (d, J = 8.8 Hz, Ar-H, 2H), 7.30 (d, J = 9.6 Hz, Ar-H, 1H), 7.29 (d, J = 9.6 Hz, Ar-H, 1H), 7.22 (d, J = 8.4 Hz, Ar-H, 2H), 2.51 (s, –CH$_3$, 3H) ppm. HRMS-FAB$^+$ (m/z): [M]$^+$ calcd for C$_{24}$H$_{14}$FNS, 367.0831; found, 367.0822.

Synthesis of 3

1,4-Bis[4-(methylsulfanyl)phenyl]ethynyl-2-fluorobenzene (3). Compound **3** was synthesized according to the general Sonogashira coupling conditions outlined for the preparation of **1b**: **1c** (0.74 mmol, 0.11 g), 1-bromo-3-fluoro-4-iodobenzene (0.37 mmol, 0.11 g), Pd(PPh$_3$)$_4$ (37 μmol, 43 mg), CuI (37 μmol, 43 mg), TEA (5 mL), and THF (5 mL); purification by column chromatography on silica gel (eluent: CHCl$_3$/hexane = 1/2, v/v), followed by recrystallisation from CHCl$_3$/hexane; colorless solid (75.3 mg, 52%). ^{1}H NMR (400 MHz, CDCl$_3$) δ 7.49–7.42 (m, Ar-H,

Table 1 DSC-derived phase-transition temperatures (°C) and enthalpy changes (ΔH in kJ mol^{-1}) obtained from heating (upper line) and cooling (lower line) scans; DSC temperature gradient: 10 °C min^{-1}

Compd	Cr–N/°C (ΔH)	N-Iso/°C (ΔH)	N range/°C
1	149.9 (18.1)	290.0[a]	140.1
	139.7 (17.5)	284.0[a]	144.3
2	179.0 (26.9)	284.3 (1.6)	104.4
	151.7 (25.3)	283.4 (1.3)	132.6
3	203.8 (35.5)	250.1 (1.3)	46.3
	192.8 (35.5)	246.4 (1.3)	53.5

[a] Observed by POM.

5H), 7.25–7.20 (m, Ar-*H*, 6H), 2.51 (s, –C*H*$_3$, 6H) ppm. HRMS-FAB$^+$ (*m/z*): [M]$^+$ calcd for $C_{24}H_{17}FNS_2$, 388.0756; found, 388.0746.

Results and discussion

The phase transition temperatures for **1–3**, determined by differential scanning calorimetry and polarized optical microscopy are summarized in Table 1, and the corresponding DSC curves are shown in Fig. S1–S3.† As shown in Table 1, **1–3** exhibit solely enantiotropic N phases without further higher-ordered smectic phases; the marble and schlieren textures indicative of N phases are shown in Fig. S4–S6.† Here, it is important to note that asymmetrically substituted **1** and **2** exhibit significantly wider N phases than symmetric **3**. Relative to the corresponding hexylsulfanyl-derivative, **3** shows a wider mesophase.[7] The melting temperatures (T_m), indicating the transition from the crystal (Cr) to the N phase, of **1** (149.9 °C) and **2** (179.0 °C) are considerably lower than that of **3** (203.8 °C). Conversely, the clearing temperatures (T_i) for **1** and **2** are higher than that for **3**, indicating a considerable expansion of the mesophases. Thus, during the heating scans, N phases were observed in the following order: 140.1 °C (**1**) > 104.4 °C (**2**) > 46.3 °C (**3**).

UV-vis absorption

The UV-vis spectra for **1**, **2**, and **3** were measured in dichloromethane (DCM) and are shown in Fig. 2. For **1** and **3**, the longest absorption edges are <400 nm, while that of **2** is ~400 nm. These results indicate that **1–3** are suitable mesogenic units for optical applications, given that they exhibit low absorption in the visible wavelength region.

Birefringence measurements

Subsequently, we evaluated the optical properties of **1–3**. For that purpose, we measured n_e, n_o, and calculated the corresponding Δn values ($\Delta n = n_e - n_o$) from target material mediums, following a previously reported method.‡[9,10] For **1**,

‡ As we could not observe clear transmittance spectra, n_e values for **3** were estimated from $n_e = \Delta n - n_o$. In this case, the temperature dependence of Δn was evaluated according to a previously described method; see: ref. 6a.
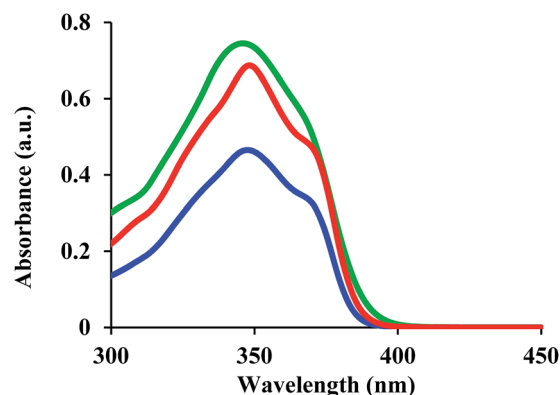

Fig. 2 UV-vis spectra for **1** (red line), **2** (green line), and **3** (blue line) in DCM.

measurements were conducted up to $T = 250$ °C, as POM measurements showed signs of decomposition beyond this temperature, most likely on account of its high T_i. The representative transmittance spectra for **1** are shown in Fig. S7 and S8.† The temperature dependence of the obtained refractive index and Δn values at 550 nm are shown in Fig. 3, where T_{IN} and T represent the transition temperatures from the isotropic
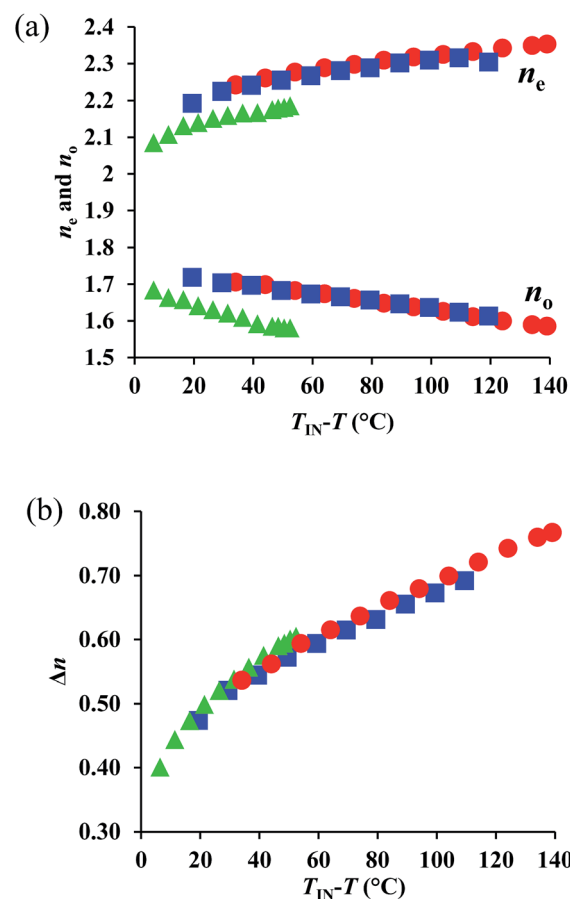

Fig. 3 Temperature dependence of (a) n_e and n_o, as well as (b) Δn values at 550 nm for **1** (red circles), **2** (red squares), and **3** (green triangles).

(Iso) liquid to the N phase and the temperature measured upon cooling, respectively. Fig. 3(a) shows that **1–3** exhibited, on account of their highly anisotropic structures, their highly polarizable substituents, and their short alkyl chains, extremely high refractive index values ($n_e > 2.1$). The corresponding value for **1** ($n_e > 2.3$) is particularly interesting, as it is close to that of diamond. From a comparison of the temperature dependence of the n_e and n_o values at $T_{IN} - T$, it is apparent that the n_e values of **1** and **2** are higher than that of **3**, whereby the value of **1** is slightly higher than that of **2**. In addition, the n_o values of **1** and **2** are also higher than that of **3**, which explains the higher mean refractive index ($\langle n \rangle$) of the former compounds with respect to the latter. The $\langle n \rangle$ values for **1** (1.84) and **2** (1.84) are comparable, and relatively high (Table 2). Fig. 3(b) illustrates the extremely high Δn values (>0.6) obtained for these compounds, which are a consequence of their high n_e values. Notably, **1** reaches a maximum ($\Delta n = 0.77$) at the lowest measurement temperature (Table 2), which is, to the best of our knowledge, the highest Δn value so far obtained from a single component system, excluding extrapolated values from room-temperature nematic mixtures. This result demonstrates the success of the present design strategy, which is based on a combination of conjugation, asymmetry, and highly polarizable substituents.

In the high-temperature region ($T_{IN} - T < 30\ °C$), the temperature dependence of Δn for **1** and **2** is similar to that of **3**. However, with increasing $T_{IN} - T$, the Δn of **3** surpasses those of **1** and **2**, despite the fact that the molecular polarizability anisotropy follows the order NCS > CN > SCH$_3$. This result implies that the Δn of **3** increases with decreasing temperature at a higher rate than those of **1** and **2**, which could be due to the enhanced S···S interactions of the two SCH$_3$ (or SR) substituents in **3** (*vide infra*).

The wave-length dependences of the Δn values at each representative temperature are shown in Fig. S9–S11,† showing positive dispersion in analogy with those for typical rod-like molecules. We compared the n_e, n_o, and Δn values for all compounds at 550 nm and 700 nm (Fig. 4). A comparison of Fig. 3 and 4 shows that the n_e, n_o, and Δn values at 770 nm are lower than those at 550 nm, due to the positive dispersion of refractive indices for **1–3**. Their temperature dependence at 700 nm exhibits a similar trend as that at 550 nm. For **1–3**, the degree of wavelength dispersion, *i.e.*, the Δn ratios at 550 nm and 700 nm (Δn (550 nm)/Δn (700 nm)), are ~1.2. The comparable UV-vis absorptions (Fig. 2) suggest that the wave-length dependence of the refractive indices should not be affected substantially.

Fig. 4 Temperature dependence of (a) n_e and n_o, as well as (b) Δn values at 700 nm for **1** (red circles), **2** (red squares), and **3** (green triangles).

WAXD measurements for the evaluation of the order parameters

Here, the temperature dependence of Δn is empirically described by the following equation: $\Delta n = S\Delta n_o$, wherein $S = (1 - T/T_i)^\beta$; Δn_o refers to Δn for the perfectly oriented state, *i.e.*, $S = 1$, while T and T_i represent measurement and clearing temperature, respectively; β is a constant characteristic for nematic materials.[11] Accordingly, Δn is proportional to the order parameter S. Considering the aforementioned temperature dependence of Δn for each compound, we speculated that the determining factor may be the order parameters of **1–3**. To examine the correlation between the order parameter and Δn, we estimated the temperature dependence of S by detailed XRD measurements using specimens aligned through an external magnetic field, which is described in detail elsewhere.[12] The obtained 2D-XRD patterns are shown in Fig. S12–S14 (ESI).† The temperature dependence of S, using this wide-angle X-ray diffraction technique (WAXD), is shown in Fig. 5. The results demonstrate that these materials exhibit high-order parameters ($S = $ ~0.5) during the isotropic to nematic transition, and $S > 0.7$ near the crystallization temperature. These values are considerably higher than those for conventional rod-like LC molecules ($S = $ ~0.3–0.6).[13] This is most likely due to the highly anisotropic structures of **1–3**, which leads to higher degrees of anisotropic

Table 2 Refractive index and birefringence values for **1–3** at the lowest measurement temperature

Compd	n_e	n_o	$\langle n \rangle^a$	Δn
1	2.35	1.59	1.84	0.77
2	2.30	1.61	1.84	0.69
3	2.19	1.58	1.78	0.61

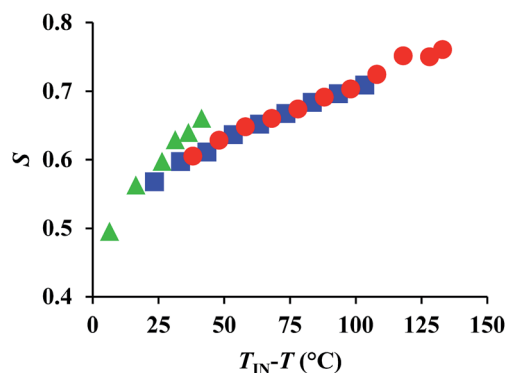^{a} $\langle n \rangle = (n_e + 2n_o)/3$.

Fig. 5   Temperature dependence of the estimated order parameter (S) obtained by WAXD measurement for **1** (red circles), **2** (blue squares), and **3** (green triangles).

interactions. The wide mesophase of **1** (140 °C) induces a particularly high S value (0.75). Conversely, a comparison of the temperature dependence suggests that with decreasing temperature, the S value for **3** is much higher than those of **1** and **2**, which means that this parameter is strongly influenced by temperature. Previously, we have reported that the optical properties of LC molecules with alkylsulfanyl groups exhibit a high temperature dependence as a consequence of the S···S interactions. Since the present results are consistent with this trend, and due to the S···S interactions between the two symmetric SCH$_3$ substituents, the Δn values for **3** should be higher than those for **1** and **2** in the low temperature region (e.g. $T_{IN} - T = 30$ °C). This result demonstrates that two symmetric SCH$_3$ or SR substituents are able to induce higher levels of S···S interactions relative to an asymmetric substitution pattern with one SCH$_3$ or SR substituent. This may lead to a higher Δn at similar $T_{IN} - T$, even though **3** exhibited in the present case, on account of its narrower mesophase, a lower maximum Δn compared to **1** and **2**.

Conclusions

In summary, we presented the design and synthesis of three bistolane-based molecules with alkylsulfanyl groups (**1–3**). These materials exhibit well-defined enantiotropic nematic phases in the absence of any smectic phases. Owing to their asymmetric structure, the transition temperatures of **1** and **2** are significantly lower, and their nematic ranges are broader than those of symmetric **3**. With respect to optical properties, it is noteworthy that **1–3** exhibit extremely high refractive indices and Δn values in their mesophases (e.g. **1** and **2**: $n_e > 2.3$; $\langle n \rangle = \sim 1.9$). At the lowest measurement temperature, **1** showed an extremely high birefringence ($\Delta n = 0.77$). Moreover, **3** exhibited, due to the presence of two SR substituents, increased levels of S···S interactions relative to **1** and **2** with asymmetric substitution patterns including one SR group. This led to the highest Δn value for **3** close to $T_{IN} - T$. Given their extremely high refractive index, these materials should find applications in various optical materials.

Notes and references

1 (a) J. W. Goodby, *Liq. Cryst.*, 2011, **38**, 1363; (b) P. Kirsh and M. Bremer, *Angew. Chem., Int. Ed.*, 2000, **39**, 4216; (c) M. Mitov, *Adv. Mater.*, 2012, **24**, 6260; (d) R. Dąbrowski, P. Kula and J. Herman, *Crystals*, 2013, **3**, 443.

2 (a) D. J. Broer, J. Lub and G. N. Mol, *Nature*, 1995, **378**, 467; (b) J. Hwang, M. H. Song, B. Park, S. Nishimura, T. Toyooka, J. W. Wu, Y. Takanishi, K. Ishikawa and H. Takezoe, *Nat. Mater.*, 2005, **4**, 383; (c) M. Funahashi and N. Tamaoki, *Mol. Cryst. Liq. Cryst.*, 2007, **475**, 123; (d) M. G. Chee, M. H. Song, D. Kim, H. Takezoe and I. J. Chung, *Jpn. J. Appl. Phys.*, 2007, **46**, L437; (e) M. Itoh, M. Tokita, H. Hegi, T. Hayakawa, S. Kang and J. Watanabe, *J. Mater. Chem.*, 2011, **21**, 1697; (f) X. Chen, L. Wang, Y. Chen, C. Li, G. Hou, X. Liu, X. Zhang, W. He and H. Yang, *Chem. Commun.*, 2014, **50**, 691; M. Uchimura, Y. Watanabe, F. Araoka, J. Watanabe, H. Takezoe and G. Konishi, *Adv. Mater.*, 2010, **22**, 4473.

3 (a) K. Okano, O. Tsutsumi, A. Shishido and T. Ikeda, *J. Am. Chem. Soc.*, 2006, **128**, 15368; (b) K. Okano, A. Shishido, O. Tsutsumi, T. Shiono and T. Ikeda, *J. Mater. Chem.*, 2005, **15**, 3395; (c) K. Okano, A. Shishido and T. Ikeda, *Adv. Mater.*, 2006, **18**, 523; (d) A. Shishido, *Polym. J.*, 2010, **42**, 525; (e) N. Kawatsuki, H. Matsushita, T. Washio, J. Kozuki, M. Kondo, T. Sasaki and H. Ono, *Macromolecules*, 2014, **47**, 324.

4 (a) H. R. Stapert, S. del Valle, E. J. K. Verstegen, B. M. I. van der Zande, J. Lub and S. Stallinga, *Adv. Funct. Mater.*, 2003, **13**, 732; (b) P. Valley, D. L. Mathine, M. R. Dodge, J. Schwiegerling, G. Peyman and N. Peyghambarian, *Opt. Lett.*, 2010, **35**, 336; (c) P. Valley, M. R. Dodge, J. Schwiegerling, G. Peyman and N. Peyghambarian, *Opt. Lett.*, 2010, **35**, 2582.

5 (a) D. Węgłowska, P. Kula and J. Herman, *RSC Adv.*, 2016, **6**, 403; (b) S. Gauza, C.-H. Wen, S.-T. Wu, N. Janarthanan and C.-S. Hsu, *Jpn. J. Appl. Phys.*, 2004, **43**, 7634; (c) C. Sekine, M. Ishitobi, K. Iwakura, M. Minai and K. Fujisawa, *Liq. Cryst.*, 2002, **29**, 355; (d) X.-L. Guan, L.-Y. Zhang, Z.-L. Zhang, Z. Shen, X.-F. Chen, X.-H. Fan and Q.-F. Zhou, *Tetrahedron*, 2009, **65**, 3728; (e) Z. Zhang, L. Zhang, X. Guan, Z. Shen, X. Chen, G. Xing, X. Fan and Q. Zhou, *Liq. Cryst.*, 2010, **37**, 69.

6 (a) Y. Arakawa, S. Nakajima, R. Ishige, M. Uchimura, S. Kang, G. Konishi and J. Watanabe, *J. Mater. Chem.*, 2012, **22**, 8394; (b) S.-T. Wu, U. Finkenzeller and V. Reiffenrath, *J. Appl. Phys.*, 1989, **65**, 4372; (c) S.-T. Wu, C.-S. Hsu and K.-F. Shyu, *Appl. Phys. Lett.*, 1999, **74**, 344; (d) A. Spadło, R. Dąbrowski, M. Filipowicz, Z. Stolarz, J. Przedmojski, S. Gauza, C. Y. H. Fan and S.-T. Wu, *Liq. Cryst.*, 2003, **30**, 191; (e) M. Hird, A. J. Seed, K. J. Toyne, J. W. Goodby, G. W. Gray and D. G. McDonnell, *J. Mater. Chem.*, 1993, **3**, 851; (f) Y.-M. Zhang, D. Wang, Z.-C. Miao, S.-K. Jin and H. Yang, *Liq. Cryst.*, 2012, **39**, 1330; (g) C. Sekine, N. Konya, M. Minai and K. Fujisawa, *Liq. Cryst.*, 2001, **28**, 1361; (h) O. Catanescu and L.-C. Chien, *Liq. Cryst.*, 2006, **33**, 115; (i)

P. Kula, J. Herman, S. Pluczyk, P. Harmata, G. Mangelinckx and J. Beeckman, *Liq. Cryst.*, 2014, **41**, 503; (*j*) D. V. Sai, P. Sathyanarayana, V. S. S. Sastry, J. Herman, P. Kula, R. Dabrowski and S. Dhara, *Liq. Cryst.*, 2014, **41**, 591; (*k*) Y. Arakawa, S. Kang, S. Nakajima, K. Sakajiri, Y. Cho, S. Kawauchi, J. Watanabe and G. Konishi, *J. Mater. Chem. C*, 2013, **1**, 8094; (*l*) Y. Arakawa, S. Nakajima, S. Kang, M. Shigeta, G. Konishi and J. Watanabe, *J. Mater. Chem.*, 2012, **22**, 13908; (*m*) Y. Arakawa, S. Nakajima, S. Kang, M. Shigeta, G. Konishi and J. Watanabe, *Liq. Cryst.*, 2012, **39**, 1063; (*n*) Y. Arakawa, S. Kang, J. Watanabe and G. Konishi, *Chem. Lett.*, 2014, **43**, 1858; (*o*) Y. Arakawa, H. Kuwahara, K. Sakajiri, S. Kang, M. Tokita and G. Konishi, *Liq. Cryst.*, 2015, **42**, 1419; (*p*) Y. Arakawa, S. Kang, J. Watanabe and G. Konishi, *Phase Transitions*, 2015, **88**, 1188; (*q*) E.-W. Lee, M. Hattori, F. Uehara, M. Tokita, S. Kawauchi, J. Watanabe and S. Kang, *J. Mater. Chem. C*, 2015, **3**, 2266; (*r*) Y.-Z. Zhao, D. Wang, Z.-M. He, G. Chen, L.-Y. Zhang, H.-Q. Zhang and H. Yang, *Chin. Chem. Lett.*, 2015, **26**, 785; (*s*) Y. Arakawa, S. Nakajima, S. Kang, G. Konishi and J. Watanabe, *J. Mater. Chem.*, 2012, **22**, 14346.

7 Y. Arakawa, S. Kang, H. Tsuji, J. Watanabe and G. Konishi, *RSC Adv.*, 2016, **6**, 16568.

8 (*a*) A. J. Seed, K. J. Toyne, J. W. Goodby and D. G. McDonnell, *J. Mater. Chem.*, 1995, **5**, 1; (*b*) A. J. Seed, K. J. Toyne and J. W. Goodby, *J. Mater. Chem.*, 1995, **5**, 2201; (*c*) G. J. Cross, A. J. Seed, K. J. Toyne, J. W. Goodby, M. Hird and M. C. Artal, *J. Mater. Chem.*, 2000, **10**, 1555; (*d*) A. J. Seed, K. J. Toyne, M. Hird and J. W. Goodby, *Liq. Cryst.*, 2012, **39**, 403; (*e*) A. J. Seed, K. Pantalone, U. M. Sharma and A. M. Grubb, *Liq. Cryst.*, 2009, **36**, 329; (*f*) Y. Arakawa, S. Kang, J. Watanabe and G. Konishi, *RSC Adv.*, 2015, **5**, 8056; (*g*) D. Węgłowska, P. Kula and J. Herman, *RSC Adv.*, 2016, **6**, 403.

9 (*a*) R. Chang, *Mol. Cryst. Liq. Cryst.*, 1974, **28**, 1; (*b*) E. Hecht, *Optics*, Addison-Wesley, Boston, 4th edn, 2002, pp. 416–425.

10 (*a*) S. Kang, S. Nakajima, Y. Arakawa, G. Konishi and J. Watanabe, *J. Mater. Chem. C*, 2013, **1**, 4222; (*b*) Y. Arakawa, S. Kang, S. Nakajima, K. Sakajiri, S. Kawauchi, J. Watanabe and G. Konishi, *Liq. Cryst.*, 2014, **41**, 642.

11 I. Haller, *Prog. Solid State Chem.*, 1975, **10**, 103.

12 (*a*) *Handbook of Liquid Crystals*, WILEY-VCH Verlag GmbH & Co. KGaA, 2014, vol. 1, pp. 317–318; (*b*) S. Kang, S. Nakajima, Y. Arakawa, M. Tokita, J. Watanabe and G. Konishi, *Polym. Chem.*, 2014, **5**, 2253; (*c*) K. Fu, M. Sone, M. Tokita and J. Watanabe, *Polym. J.*, 2006, **38**, 442.

13 (*a*) I. Dierking, *Textures of Liquid Crystals*, WILEY-VCH Verlag GmbH & Co. KGaA, 2003; (*b*) D. H. Chen and G. R. Luckhurst, *Trans. Faraday Soc.*, 1969, **65**, 656.